

Fabrication and Characterization of Well-Aligned $Zn_{1-x}Mn_xO$ Nanorods

This article has been downloaded from IOPscience. Please scroll down to see the full text article.

2006 Chinese Phys. Lett. 23 716

(<http://iopscience.iop.org/0256-307X/23/3/053>)

View [the table of contents for this issue](#), or go to the [journal homepage](#) for more

Download details:

IP Address: 130.56.107.38

The article was downloaded on 28/03/2013 at 07:59

Please note that [terms and conditions apply](#).

Fabrication and Characterization of Well-Aligned $Zn_{1-x}Mn_xO$ Nanorods *CHANG Yong-Qin(常永勤)^{1*}, ZHANG Hong-Zhou(张洪洲)², LONG Yi(龙毅)¹, YE Rong-Chang(叶荣昌)¹¹*School of Materials Science and Engineering, University of Science and Technology Beijing, Beijing 100083*²*Department of Electronics and Material Engineering, Research School of Physical Science and Engineering, Australian National University, Australia*

(Received 18 November 2005)

Well-aligned $Zn_{1-x}Mn_xO$ nanorods have been synthesized successfully on bare silicon substrates by a simple evaporation method without using any catalyst. X-ray diffraction and electron microscopy studies demonstrate that the as-grown nanorods are of single wurtzite phase with a preferential growth direction along their c -axes. Quantitative energy-dispersive spectrum analysis reveals that the concentration of manganese is around 4 at.%. Magnetic measurements show the single-phase $Zn_{1-x}Mn_xO$ nanorod arrays exhibiting the paramagnetic behaviour. Photoluminescence spectra demonstrate that the $Zn_{1-x}Mn_xO$ nanorods preserve ultraviolet emission at room temperature.

PACS: 81.07.BC, 68.37.Lp, 75.75.+a, 78.55.Et

Nano-scaled semiconductors have attracted much attention because of their unique physical and chemical properties originating from quantum confinement effects and their potential applications in nanodevices. Considerable research works have been performed in fabrication and characterization of nano-scaled diluted magnetic semiconductors (DMSs) for spintronic devices.^[1-3] As an oxide DMS, ZnO based DMS is one of the most versatile and attractive DMSs. ZnO is widely recognized as a promising opto-material working in the blue-ultraviolet region due to its direct band gap of 3.37 eV at room temperature and a large exciton binding energy of 60 meV.^[4] With a high thermal solubility of Mn in ZnO (> 10 at.%), Mn doped ZnO is an ideal material for shot-wave magneto-optical devices and transparent magnets.^[5] Recently, Dietl *et al.*^[6] predicted that p-type Mn doped ZnO can be ferromagnetic with high Curie temperature above room temperature. Most of the previous studies on $Zn_{1-x}Mn_xO$ have been focused on ceramics and films.^[7-9] Only a few reports exist concerning $Zn_{1-x}Mn_xO$ nanowires,^[10] nanobelts,^[11] and tetrapod structures.^[12] However, for practical purposes, high-density and well-aligned nanostructures are of importance. In this Letter, a catalyst-free method for the growth of well-aligned $Zn_{1-x}Mn_xO$ nanorods is described, and their photoluminescence and magnetic properties are also discussed in detail.

Synthesis of $Zn_{1-x}Mn_xO$ nanorod arrays was conducted via a thermal evaporation of ZnO/C (mole ratio 1:1) and Mn powders without addition of any catalyst. It is worth mentioning that C acts as an effective reductive agent and assists the growth of ZnO nanostructures.^[13] The powders were placed in

a quartz tube and near one end of the tube; and near the other end, bare n-type (100)-oriented Si substrates were placed for deposition of the nanorod array (the silicon substrates had been ultrasonically cleaned in acetone and ethanol for 10 min, respectively, and rinsed in distilled water). The quartz tube was then put into a horizontal furnace and heated to 1160°C in an argon atmosphere. Here, the temperature was of the mixture powders, i.e. the source materials, and a temperature gradient between the source materials and the substrates was approximately 400°C. The evaporation lasted for 90 min. After the system cooled down to room temperature naturally, the silicon substrates were covered with a layer of weak yellow colour.

The morphology, microstructure and chemical composition of the samples were investigated by a scanning electron microscope (SEM) and a transmission electron microscope (TEM) equipped with an energy-dispersive spectrum (EDS) attachment. The phase of the samples was identified by using an x-ray diffractometer (XRD) with Cu K_α radiation and a graphitic monochromator. Raman spectra of the samples were collected at room temperature excited by an Ar⁺ laser with the wavelength of 514.5 nm. Room-temperature photoluminescence (PL) properties of the samples were investigated using a 325-nm He-Cd laser. The magnetic measurements of the samples were also carried out by means of a superconducting quantum interference device (SQUID) magnetometer.

The crystal structure and crystallographic orientation of the samples were investigated by using XRD measurement. As shown in Fig. 1, the positions of all diffraction peaks from the sample coincide with those of a hexagonal wurtzite ZnO structure (PDF 80-0075),

* Supported by the National Natural Science Foundation of China under Grant No 50502005, and Beijing Natural Science Foundation under Grant No 1062008.

** Email: yqchang@mater.ustb.edu.cn

©2005 Chinese Physical Society and IOP Publishing Ltd

while intensity of the (002) peak is quite stronger, indicating that the nanorods have well-aligned on the silicon surface and show a preferential growth direction of (002). No other peaks corresponding to manganese metal or manganese oxides were detected.

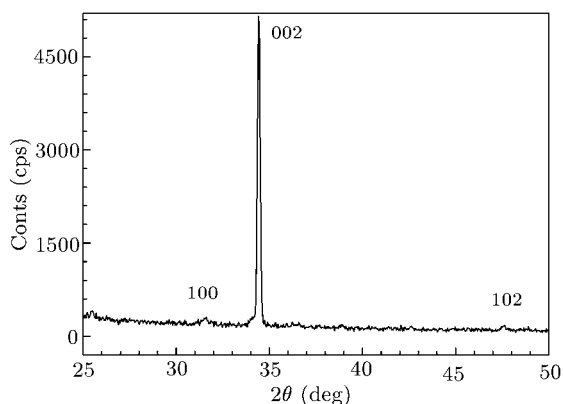


Fig. 1. XRD pattern of the $Zn_{1-x}Mn_xO$ nanorod arrays deposited on a bared silicon substrate.

Figure 2(a) presents an SEM image of the sam-

ples and it reveals that high-density and well-aligned nanorods were grown directly on the bare surface of the silicon substrate. The diameters of the nanorods are in the range of 300–500 nm, and the nanorods have round tips. To further study their structure and composition, we scratched and dispersed the nanorods onto a copper grid for TEM investigation. The bright field TEM image (Fig. 2(b)) shows an individual nanorod. Its diameter and length are 400 nm and 4 μm , respectively, and the nanorod is straight in morphology, uniform in size. A selected area electron diffraction (SAED) pattern of the nanorod is also shown by the inset in Fig. 2(b), demonstrating that the nanorod is of high crystalline perfection with a hexagonal structure. Figure 2(c) shows a high-resolution TEM image taken from the edge of a nanorod. The continuous lattice fringes demonstrate that the nanorod is almost defect-free. The measured spacing of 0.258 nm reveals that the nanorod grows along the c axis, in accordance with the XRD results shown in Fig. 1. The composition microanalysis by EDS for a single nanorod is shown in Fig. 2(d), and

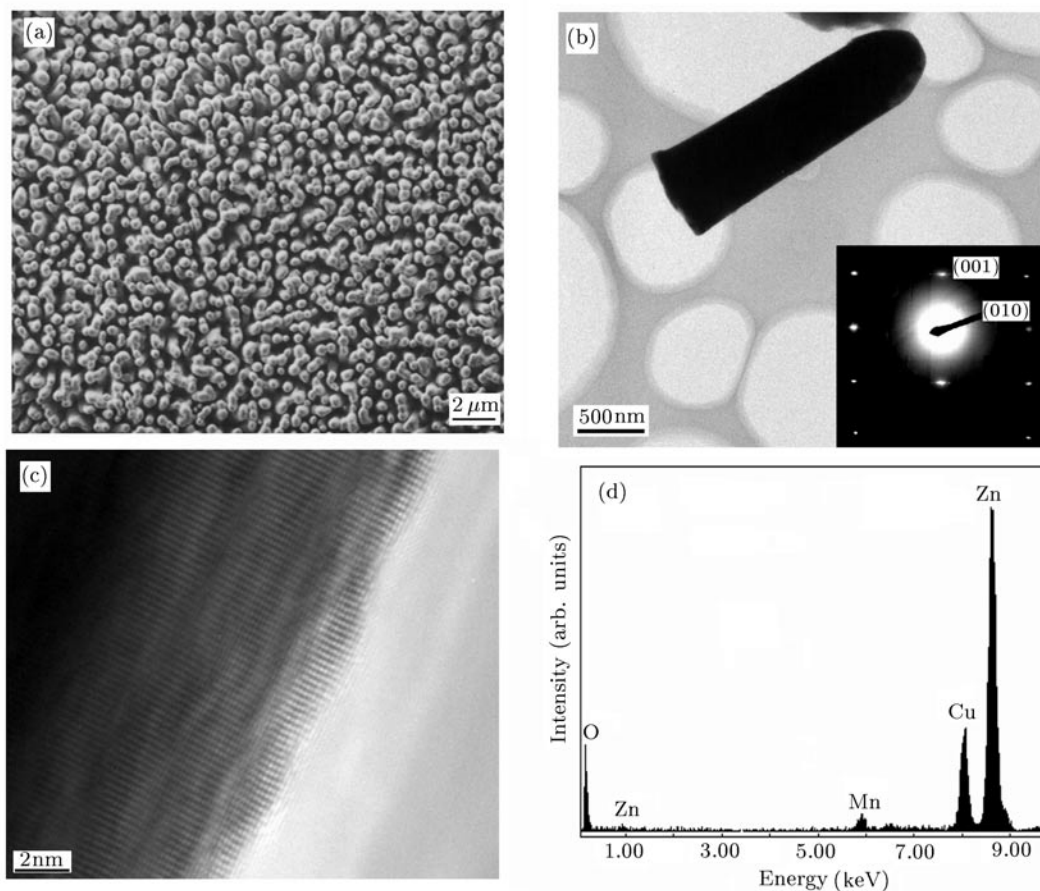


Fig. 2. (a) Top-view SEM image of the well-aligned $Zn_{1-x}Mn_xO$ nanorods on a silicon substrate. (b) Bright-field TEM image of a single $Zn_{1-x}Mn_xO$ nanorod with the diameter of 400 nm. Inset: the corresponding SAED patterns. (c) HRTEM image of a single $Zn_{1-x}Mn_xO$ nanorod. (d) Typical EDS pattern of an individual $Zn_{1-x}Mn_xO$ nanorod.

it demonstrates that the nanorod is composed of Zn, Mn and O (Cu signals are most likely ascribed to the supporting copper grid). Quantitative EDS analysis shows that the concentration of manganese is about 4 at.%.

Raman scattering spectroscopy has been employed to confirm the structures of $\text{Zn}_{1-x}\text{Mn}_x\text{O}$ nanorods. ZnO has a wurtzite structure with C_{6v} point group symmetry. Group theory predicts that it has $2A_1$, $2E_1$, $2E_2$ and $2B_1$ modes^[14–17] and only $2B_1$ modes are Raman silent. Moreover, A_1 and E_1 are polar modes and can be split into LO and TO components. A typical Raman spectrum of $\text{Zn}_{1-x}\text{Mn}_x\text{O}$ arrays deposited on silicon substrates is shown in Fig. 3. Within the Raman shift range $270\text{--}700\text{ cm}^{-1}$, the Raman bands with principal phonon lines centred at 434.0 cm^{-1} $E_{2(\text{High})}$ and 568.0 cm^{-1} $A_{1(\text{LO})}$ are characteristics of a hexagonal wurtzite phase, which can be thus assigned to the nanorods. In this Raman shift range, a strong Si peak (520.2 cm^{-1}) originating from the substrate can also be observed and serves as a reference. The Raman spectrum obviously shows that the $\text{Zn}_{1-x}\text{Mn}_x\text{O}$ nanorods keep the crystal structure of ZnO and the manganese ions incorporate into the lattice positions of ZnO through substitution of Zn atoms. In the case of highly ordered ZnO films, only $A_1(\text{LO})$ and E_2 modes are observed and the other modes are forbidden under backscattering geometry according to the Raman selection rules. The present work only shows the two bands corresponding to the $A_1(\text{LO})$ and E_2 modes, which further confirms that these arrays are highly *c*-axis oriented. Therefore, all the results of SEM, HRTEM, XRD, and Raman experiments agree well with one another and demonstrate that the deposits on silicon substrates are well-aligned *c*-oriented single phase wurtzite $\text{Zn}_{1-x}\text{Mn}_x\text{O}$ nanorods.

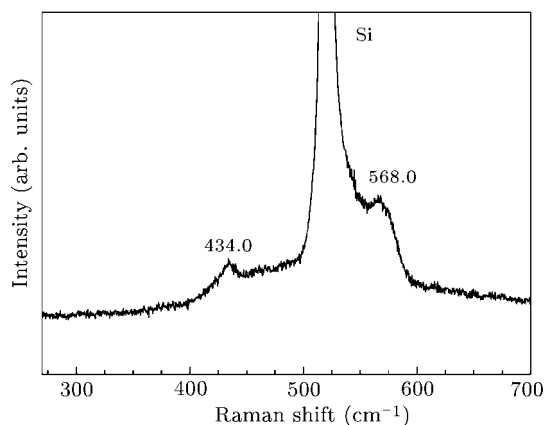


Fig. 3. Raman spectrum of the $\text{Zn}_{1-x}\text{Mn}_x\text{O}$ nanorod arrays taken at room temperature.

Figure 4(a) presents the temperature dependence of magnetization under an applied magnetic field of

500 Oe for the samples. Although un-doped ZnO exhibits diamagnetic behaviour and its magnetic susceptibility is $-46.0 (4\pi \times 10^{-6}\text{ cm}^3\text{g}^{-1})$, positive magnetization is observed from the Mn doped ZnO nanorods (the M - T curve was obtained after appropriate correction for the diamagnetic component arising from the silicon substrate). In the temperature range of $50\text{--}300\text{ K}$, the magnetization of the sample increases slowly as the temperature decreases, while a steep increase of the magnetization occurs as the temperature is below 50 K . Figure 4(b) shows the M^{-1} - T curve fitted by the Curie-Weiss law. They clearly demonstrate that the single-phase sample exhibits paramagnetic Curie-Weiss behaviour with antiferromagnetic interactions, similar to other DMSs. The result also indicates that no evidence of ferromagnetic behaviour is obtained in the intrinsic and non-carrier doped $\text{Zn}_{1-x}\text{Mn}_x\text{O}$ nanorods. Further work is needed to understand the effects leading to ferromagnetic behaviour in $\text{Zn}_{1-x}\text{Mn}_x\text{O}$ nanostructures, so that they may be optimized for future device applications.

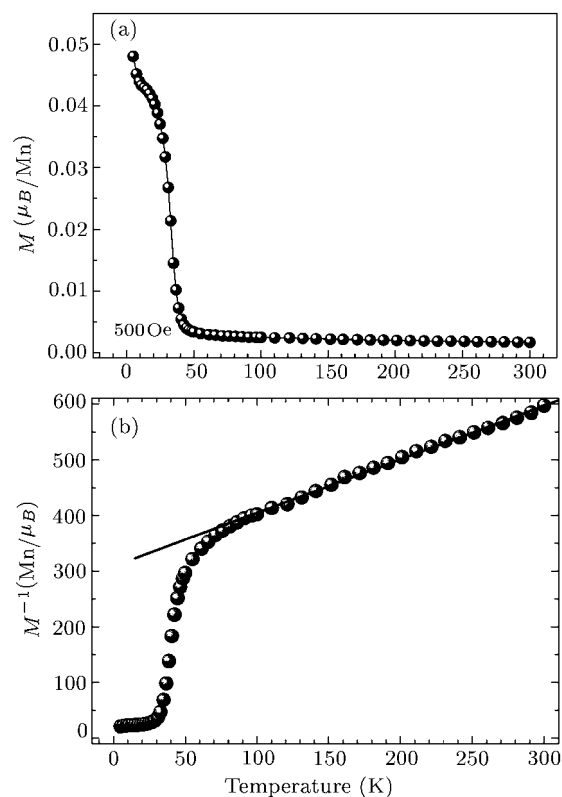


Fig. 4. (a) Temperature-dependence of magnetization (M - T) curve of the $\text{Zn}_{1-x}\text{Mn}_x\text{O}$ nanorod arrays under a magnetic field of 500 Oe (in units of μ_B per Mn atom). (b) M^{-1} - T behaviour fitted by the Curie-Weiss law.

Room-temperature photoluminescence (PL) spectra of the $\text{Zn}_{1-x}\text{Mn}_x\text{O}$ nanorods are shown in Fig. 5. Similar to the spectra of pure ZnO,^[18] the ultraviolet emission centred at 379.1 nm is related to the near band-edge transition, and the broad green emis-

sion band centred at 510.5 nm might be ascribed to the defects on the nanorods surfaces.^[19] The ultraviolet emission still preserved with the adding of manganese demonstrates that the well-aligned $\text{Zn}_{1-x}\text{Mn}_x\text{O}$ nanorods are an ideal system for the application of shot-wave magneto-optical devices.

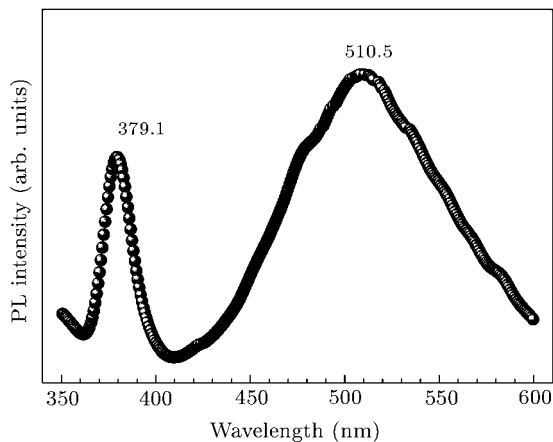


Fig. 5. Typical room-temperature photoluminescence spectrum of the $\text{Zn}_{1-x}\text{Mn}_x\text{O}$ nanorod arrays.

In summary, large-scale well-aligned $\text{Zn}_{1-x}\text{Mn}_x\text{O}$ nanorods deposited on bare silicon substrates have been prepared via a simple vapor phase growth without using any catalyst. The highly crystallized nanorods show single wurtzite phase with a preferential growth direction along their c axes. Direct-current magnetization measurements show that the single-phase $\text{Zn}_{1-x}\text{Mn}_x\text{O}$ arrays exhibit paramagnetic Curie–Weiss behaviour. Room-temperature photoluminescence spectra demonstrate an ultraviolet emission peak centred at 379.1 nm and a green emission peak broadened at 510.5 nm. With the advantages of low cost, no catalyst and scale-up production, this preparation method is a useful way for the doped compounds with well-controlled shape, which is very im-

portant to both the fundamental research and technological applications of nanodevices.

References

- [1] Kyrychenko F V and Kossut J 2001 *Physica E* **10** 378
- [2] Ge S H, Wang X W, Kou X M, Zhou X Y, Xi L, Zuo Y L, Yang X L and Zhao Y X 2005 *Chin. Phys. Lett.* **22** 1772
- [3] Takabayashi K, Takahashi N, Yagi I, Yui K, Souma I, Shen J X and Oka Y 2000 *J. Lumin.* **87-89** 347
- [4] Tang Z K, Yu P, Wong G K L, Kawasaki M, Ohtomo A, Koinuma H and Segawa Y 1997 *Solid State Commun.* **103** 459
- [5] Bates C H, White W B and Roy R 1966 *J. Inorg. Nucl. Chem.* **28** 397
- [6] Dietl T, Ohno H, Matsukura F, Cibert J and Ferrand D 2000 *Science* **287** 1019
- [7] Ando K, Saito H, Jin Z W and Fukumura T 2001 *J. Appl. Phys.* **89** 7284
- [8] Ueda K, Tabata H and Kawai T 2001 *Appl. Phys. Lett.* **79** 988
- [9] Sharma P, Gupta A, Rao K V, Owens F J, Sharma R, Ahuja R, Guillen J M O, Johansson B and Gehring G A 2003 *Nature Mater.* **2** 673
- [10] Chang Y Q, Wang D B, Xu J, Luo X H, Xu X Y, Chen C P, Wang R M and Yu D P 2003 *Appl. Phys. Lett.* **83** 4020
- [11] Ronning C, Cao P X, Ding Y, Wang Z L and Schwen D 2004 *Appl. Phys. Lett.* **84** 783
- [12] Roy V A, Djuricic A B, Zhang X X, Leung Y H, Xie M H, Gao J, Lui H F and Surya C 2004 *Appl. Phys. Lett.* **84** 756
- [13] Yao B D, Chan Y F and Wang N 2002 *Appl. Phys. Lett.* **81** 757
- [14] Madelung O 1982 *Landolt-boernstein* (Berlin: Springer) New Series, Group III, 17b, p 35
- [15] Damen T C, Porto S P and Tell B 1966 *Phys. Rev.* **142** 570
- [16] Sharma S K and Exarhos G J 1997 *Solid Stat. Phenom.* **55** 32
- [17] Zhang Z C, Huang B L, Yu L Q and Cui D L 2001 *Mater. Sci. Engin. B* **86** 109
- [18] Jeong S H, Kim B S and Lee B T 2003 *Appl. Phys. Lett.* **82** 2625
- [19] Tiwari A, Jin C, Kvit A, Kumar D, Muth J F and Narayan J 2002 *Solid Stat. Commun.* **121** 371